Brief Communication

Computational prediction of small molecules with predicted binding to FGFR3 and testing biological effects in bone cells

Subburaman Mohan[1,2,3], Karthikeyan Muthusamy[4], Selvaraman Nagamani[4] and Chandrasekhar Kesavan[1,2]

[1]Musculoskeletal Disease Center, VA Loma Linda Healthcare System, Loma Linda, CA 92357, USA; [2]Department of Medicine, Loma Linda University, Loma Linda, CA 92354, USA; [3]Department of Orthopedic Surgery, Loma Linda University, Loma Linda, CA 92354, USA; [4]Department of Bioinformatics, Alagappa University, Karaikudi 630 004, India
Corresponding author: Chandrasekhar Kesavan. Email: Chandrasekhar.Kesavan@va.gov

Impact statement

Impaired bone healing is a significant healthcare issue. Therefore, identifying small molecules that stimulate signaling pathways involved in promoting bone formation could be of therapeutic value in promoting healing of delayed fracture unions. FGFR3 is known to mediate the anabolic effects of FGFs in bone. In this study using a computational approach, we identified novel compounds predicted to bind to FGFR3. We have also established evidence that one of the identified compounds promoted proliferation and differentiation of osteogenic cells *in vitro*. Additionally, the compound increased mineralization, and expression of bone markers in *ex vivo* organ cultures demonstrating the potential of the identified compound for the therapeutic agent development.

Abstract

Activating anabolic receptor-mediated signaling is essential for stimulating new bone formation and for promoting bone healing in humans. Fibroblast growth factor receptor (FGFR) 3 is reported to be an important positive regulator of osteogenesis. Presently, recombinant proteins are used to stimulate FGFR3 function but have limitations for therapy due to expense and stability. Therefore, there is a need for identification of novel small molecules binding to FGFR3 that promote biological function. *In silico* molecular docking and high-throughput virtual screening on zinc database identified seven compounds predicted to bind to an active site within the βC'-βE loop, specific to FGFR3. All seven compounds fall within an acceptable range of ADME/T properties. Four compounds showed a 30–65% oral absorption rate. Density functional theory analysis revealed a high HOMO-LUMO gap, reflecting high molecular stability for compounds 14977614 and 13509082. Five compounds exhibited mutagenicity, while the other three compounds presented irritability. Computational mutagenesis predicted that mutating G322 affected compound binding to FGFR3. Molecular dynamics simulation revealed compound 14977614 is stable in binding to FGFR3. Furthermore, compound 14977614, with an oral absorption rate of 60% and high molecular stability, produced significant increases in both proliferation and differentiation of bone marrow stromal cells *in vitro*. Anti-FGFR3 treatment completely blocked the stimulatory effect of 14977614 on BMSC proliferation. *Ex vivo* treatment of mouse calvaria in organ culture for seven days with 14977614 increased mineralization and expression levels of bone formation markers. In conclusion, computational analyses identified seven compounds that bind to the FGFR3, and *in vitro* studies showed that compound 14977614 exerts significant biological effects on osteogenic cells.

Keywords: *In silico*, FGFR3, small molecule therapeutics, proliferation, virtual screening, alkaline phosphatase activity

Introduction

Bone healing is mediated by multiple growth factors which include, insulin-like growth factor, bone morphogenetic proteins (BMPs), fibroblast growth factor (FGF), wingless-related integration site (Wnt), etc. These growth factors promote anabolic effects through interaction with cell surface receptors that stimulate receptor-mediated-signaling pathways leading to activation of various cellular processes which promote new bone formation.[1–6] Among the growth factors studied, we focused on fibroblast growth factors (FGF)/fibroblast growth factor receptor (FGFR) 3, key players in skeletal development and maintenance based on the following experimental evidence: (1) FGFR3 is expressed by osteoblasts and periosteal cells, osteocytes, and osteoclasts.[4] (2) FGFR3 activates phosphoinositide 3-kineases, and extra-cellular signal-related kinases signaling pathways, which are essential for increasing cell number, function, and survival of bone cells.[7]

(3) Loss-of-function and gain-of-function mutations of FGFR3 resulted in osteopenia, suggesting a complex mechanism underlying the role of FGFR3 in osteogenesis.[8] (3) Mice deficient in FGFR3 showed decreased bone mineral density and osteopenia and that mice deficient in FGFR3 in osteoclast lineage cells showed impaired bone resorption.[9] Additionally, reports have shown that FGFR3 is highly expressed at the fracture site.[10] Taken together, these data demonstrate that FGFR3 is a positive regulator of osteogenesis.

Currently, specific FGF ligands in the form of recombinant proteins are used to stimulate FGFR3 signaling and treat diseases; however, the recombinant protein is not stable and is expensive. Additionally, use of a viral approach to express FGFR3 is often not acceptable to patients. Therefore, there is a need for identification of new factors that are stable, able to stimulate anabolic effect via FGFR3 signaling like FGF ligands, and are not expensive. In an effort to identify novel therapeutics, we focused on discovering small molecule agonists of the FGFR3 that are safe and can be produced in large quantities at a fraction of cost compared to recombinant FGFs. To identify small molecule therapeutics that could stimulate FGFR3 signaling, we carried out computational analysis to identify potential FGFR3 agonists and subsequently tested their biological activity in bone cells *in vitro*.

Materials and methods

Protein structure preparation and receptor grid preparation

All computational studies were carried out using Schrodinger, LLC, New York, 2015–4 software package. The FGFR3 protein structure was downloaded from the Protein Data Bank (PDB id−1RY7) in a complex with FGF1. The FGF1 structure was removed from the FGF1-FGFR3 complex.[11] The ligand binding site's characteristics and FGFR3 protein active site were examined using the SiteMap program (Version 3.6, Schrodinger, 2016).

Database and high throughput virtual screening

Virtual screening workflow program (Schrödinger, LLC, New York, 2009) includes Ligprep (for ligand preparation), absorption, distribution, metabolism, excretion, toxicity (ADME/T) predicted by Qikprop (Version 4.8, Schrondinger, 2016), HTVS (high throughput virtual screening), and structural properties were used to screen compounds with potential binding properties to FGFR3 from the zinc database.[12,13]

Density functional theory and toxicity risk assessment

Density functional theory (DFT) was performed on the identified compounds through Becke's three-parameter exchange potential and Lee-Yang-Parr correlation functional (B3LYP), using Poisson Boltzmann finite (PBF) solvation.[14] The lead molecules analyzed by qikprop were further evaluated for toxicity and drug likeness properties with OSIRIS Property Explorer software (https://www.organic-chemistry.org/prog/peo/).

Computational mutagenesis studies and molecular dynamics simulations

Computational mutagenesis and alanine scanning studies were performed using the Mutate Residues script available in Schrodinger, LLC, New York, NY, USA. The contribution of specific residues to the protein function was calculated by computational mutagenesis studies.[15] Furthermore, the best protein ligand complex (FGFR3_14977614) given as input for molecular dynamics (MD) simulations. The MD simulations was carried out in GROMACS with the united atom united atom Gromos9643a1 force field in NVT and NPT environment under the periodic boundary conditions. The ligand topology and coordinate file were generated externally using PRODRG server.[16] The complex has been placed inside the cubic box with simple point charge water model. The dimension of the cubic is $11.23 \times 12.43 \times 11.56$ (all in Å). In order to make the model system neutral, we have added six chlorine ions at random positions. The whole system was minimized using steepest descent method with 50,000 minimization and tolerance of 1000 kJ $mol^{-1}nm^{-1}$. Particle mesh Ewald (PME) method was applied for the electrostatic and van der Waals (vdW) interactions with a cutoff distance of 1.0 nm for short-range neighbor list (rlsit) and 1.0 nm for coulomb cutoff (rcoulomb) and 1.0 nm for the vdW interactions.

Cell culture, proliferation, and ALP assays

Bone marrow stromal cells (BMSCs) from the long bones were obtained from each euthanized mice (six-month-old C57BL/6J mice, $n = 5$) and cultured in αMEM media containing 10% fetal bovine serum and antibiotics as described.[17] The first passage cells were used for the experiment.[18] Approximately 4000 cells were plated per well in α minimal essential medium (αMEM) containing 10% fetal calf serum and antibiotics for the assay. After 48 h of incubation, cells were serum deprived in αMEM containing 0.1% bovine serum albumin and antibiotics for 24 h at 37°C in the CO_2 incubator. Fresh serum-free medium was added, and cells were incubated with 14977614 at 1 or 10 μM prior to termination after 48 h of treatment for the cell proliferation assay. The proliferation assay was performed using Cy-Quant Dye (Thermo Fisher Scientific, USA) according to the manufacturer's instructions. For alkaline phosphatase (ALP) staining, the cells were cultured in differentiation media containing 50 μg/mL ascorbic acid and 10 mM β-glycerophosphate. The media with 14976614 was changed at two-day intervals. The study was terminated nine days post treatment. ALPs staining was performed using an ALP kit (Sigma, USA). For quantitation of ALP staining, the cells were washed with 1× phosphate buffer and 100 μL dimethyl sulfoxide (DMSO) was added to each well and quantitated at 590 nM using a plate reader (BioTek Instruments Inc., USA).

Calvaria culture, osteomeasure mineralization, and gene expression

Calvaria were isolated from one-week-old C57BL/6J mice ($n = 3$ mice/group) for two different experiments. A 3 mm circular calvaria disc was prepared using a hole punch. We used calvaria from the same mice and the hole punch was created in a similar position on the calvaria for vehicle and drug treatment to minimize variation in the data. The calvaria were cultured in αMEM with antibiotics and 100 μM 14977614 for seven days. The media and drug were changed every day. Seven days post treatment, the first group was stained for mineralization using an osteomeasure Image mineralization kit (Lonza, USA) according to the manufacturer's instructions. The fluorescence in each calvaria (treated and untreated) were semi-quantitatively assessed by Fiji software (open-source platform for biological-image analysis). The complete calvaria region was selected for the analysis. The software provides values area, integrated values (reflecting fluorescence) subtracted from background (area with no fluorescence). The second group was subjected to total RNA isolation, reverse transcription, and gene expression analysis using real-time PCR. β-actin was used as an internal control to normalize the data.[19]

Cell proliferation with 14977614, anti-FGFR3, IgG control, and FGF1 ligand

BMSCs isolated from euthanized six-month-old C57BL/6J male mice were pooled and cultured in αMEM media containing 10% fetal bovine serum. The second passage cells were used for the experiment. Approximately 5000 cells were plated per well in αMEM containing 10% fetal calf serum and antibiotics for the assay. After 48 h of incubation, cells were serum deprived in αMEM containing 0.1% bovine serum albumin and antibiotics for 24 h at 37°C in the CO_2 incubator. Fresh serum-free medium was added, and cells were pre-treated for 1 h with 1 μg/mL of mouse anti-FGFR3 rat monoclonal antibody (R&D Systems, Minneapolis, MN) or 1 μg/mL of normal rat IgG prior to incubation with vehicle (1× PBS), 30 μM of 14977614 or 20 ng/mL of FGF1. The study was terminated 48 h later for the cell proliferation assay.

Results and discussion

In silico molecular docking analysis revealed seven compounds predicted to bind to the active site of FGFR3 protein (Table 1) Compound 76945126 exhibited the highest binding affinity, while compounds 14977614 and 13509082

Table 1. Docking results and ADME/T (adsorption, distribution, metabolization, excretion, and toxicity) analyses of the screened compounds against FGFR3.

Docking results and ADME/T analysis	Parameters	Compounds[a]						
		1	2	3	4	5	6	7
	Glide docking score[b]	−10.09	−7.74	−7.69	−7.36	−7.29	−7.06	−7.00
	Glide docking energy[c]	−61.54	−53.43	−35.53	−60.08	−46.73	−47.91	−43.11
	Mol_Wt[d]	665.44	421.45	262.22	488.54	308.29	308.29	384.40
	QPLogpw[e]	39.27	23.23	18.78	29.58	23.17	14.90	24.71
	QPLog po/w[f]	−3.09	0.36	−1.38	−4.64	−1.68	1.65	−3.39
	Rule of five[g]	3	0	1	2	1	0	2
	QPLog HERG[h]	−2.37	−3.32	−5.10	3.56	−5.20	−7.75	−3.74
	% of human oral absorption[i]	0	50.47	21.32	0	30.11	65.34	0
	HOMO[j]	−0.17	−0.22	−0.22	−0.17	−0.21	−0.23	−0.22
	LUMO[k]	−0.03	−0.11	−0.10	−0.02	−0.07	−0.03	−0.02
	HLG[l]	−0.14	−0.11	−0.12	−0.15	−0.14	−0.20	−0.20
Toxicity risk	*MUT*	LR	LR	HR	LR	MR	LR	LR
	IRRI	LR	LR	LR	MR	MR	HR	LR
	REP	LR	LR	MR	LR	HR	LR	LR
	CLP	−5.32	−5.37	−5.12	−5.35	−5.27	−6.11	−4.45
Drug-likeness	*S*	−1.29	−0.39	−1.02	−2.37	1.26	2.83	−0.71
	TPSA	235	221	2354	242	235	321	204
	DL	1.01	−1.24	−1.17	−1.75	−0.04	−12.03	−1.16
	DS	0.61	0.52	0.26	0.27	0.24	0.08	0.5

Note: Compounds are list as 1-76945126; 2-63818502; 3-01827214; 4-25725679; 5-15774975, 6-14977614 and 7-13509082.
MUT: mutagenicity; *IRRI*: irritation; *REP*: reproduction; *CLP*: ClogP; *S*: solubility; *TPSA*: topological polar surface area; *DL*: druglikeness; *DS*: drug score; *LR*: low risk; *MR*: medium risk; *HR*: high risk.
[a]Zinc database compound id.
[b]Glide score based on the chemscore.
[c]Binding energy calculated while docking and binding free energy.
[d]Molecular weight of the molecule. −130.0 – 725.0.
[e]Predicted water/gas partition coefficient. 4.0 – 45.0.
[f]Predicted octanol/water partition coefficient. −2.0 – 6.5.
[g]Lipinski rule of five—Maximum is four.
[h]Predicted IC50 value for blockage of HERG K+ channels—Concern below −5.
[i]Predicted human oral absorption on 0 to 100% scale – >80% is high, <25% is poor.
[j]Highest occupied molecular orbital.
[k]Lowest unoccupied molecular orbital.
[l]HLG – HOMO – LUMO Gap.

showed a weak binding affinity to the FGFR3 protein. The rest of the compounds (63818502, 01827214, 25725679, and 15774975) showed a moderate binding affinity. To further characterize the physiochemical properties (ADME/T) of the compounds, Qikprop calculation was performed on the identified compounds using the Schrodinger software. The molecular weight, lipophilicity, and drug-likeness score (a combination of CloP, LogS, TPSA analysis) for the identified compounds were within the acceptable standard range. Four compounds (63818502, 01827214, 15774975, and 14977614) showed a predicted human oral absorption rate, while compounds 25725679, 13509082, and 76945126 have an unmeasurable oral absorption rate, suggesting that these compounds need special modifications to improve oral absorption (Table 1). Density functional theory analysis revealed that compounds 14977614 and 13509082 showed a

high HUMO (highest occupied molecular orbital) -LUMO (lowest unoccupied molecular orbital) gap (−0.20), while others showed modest HUMO-LUMO gap (−0.14–0.17) (Table 1) suggesting that 14977614 and 13509082 were highly stable compared to the other identified compounds. Toxicity prediction on the identified compounds revealed varying levels of risk for toxicity, mutagenesis, and irritability as shown in Table 1. In summary, all seven compounds are within an ADME/T acceptable range defined for human use, indicating their potential for use as drug-like molecules.

Structural data from FGFR3 indicated that the amino acids in the βC′-βE loop, located in the C-terminal of the FGFR3 plays an important role in ligand binding (for example, FGF1, FGF18) and varies in the amino acids number between the FGFR family members due to alternate
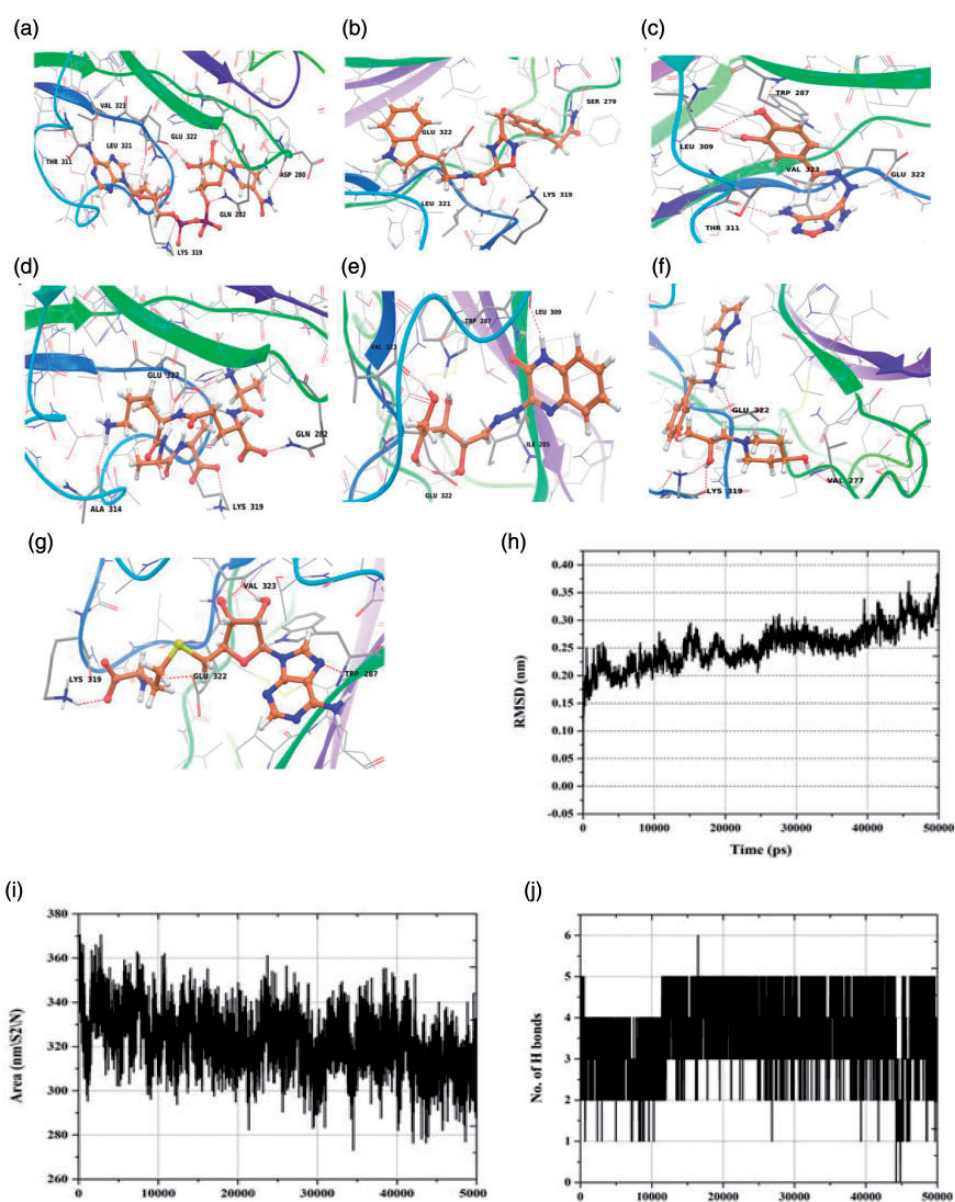

Figure 1. (a–g) The 2D representation of the identified small molecules binding to amino acids located in the active site of FGFR3. a–g corresponds to compounds, a-76945126, b-63818502, c-01827214, d-25725679, e-15774975, f-14977614, and g-13509082 and backbone RMSD (h) backbone RMSD, (i) Solvent accessible surface area, and (j) number of hydrogen bonds of best compound 14977614 in the active site of FGFR3. (A color version of this figure is available in the online journal.)

splicing suggesting a mechanism whereby ligand binding specificity occurs from difference in tertiary folding of FGFR3. Therefore, we carried out a ligand binding specificity computational analysis by tabulating the hydrogen bond interactions and distances to determine if the identified compounds bind to the amino acids of the βC'-βE loop of FGFR3 where natural ligands that act as an agonist (FGF1, FGF18) interact with FGFR3. Our analysis found that the identified compounds bound to amino acids in this region through hydrogen bonding, in particular to Glu-322, which is specific to FGFR3 in the FGFR family and falls within the βC'-βE loop. Based on this result, we conclude that the identified compound may function as an agonist. We also found that the identified compounds showed interactions with other amino acids (Figure 1(a) to (g)). While these data show that the compounds differ in the number of amino acids with which they interact in the FGFR3 ligand binding site, it is yet to be determined whether these differences in amino acid interactions contribute to differences in stimulating FGFR3 signaling and thereby biological activity.

To further explore the importance of compound interaction with amino acids in the active site of FGFR3, we replaced the specific amino acids with alanine and evaluated the protein-compound interaction by computational mutagenesis for the two compounds. In the FGFR3-14977614 complex and in the FGFR3-63818502 complex, the ΔGbind[a] energy was 112.46 kcal/mol and 126.48 kcal/mol, respectively, in the wild type (WT) interaction. When the interacting amino acids (V277A, S279A, L319A, L321A, and G322A) of FGFR3 with the compounds were mutated,

we found a reduction in the ΔGbind[a] energy, ΔGbind$_{covalent}$, ΔGbind$_{Hbond}$, ΔGbind$_{Lipo}$, ΔGbind$_{SolvGB}$ (Table 2) for all amino acids suggesting that all amino acids are essential for binding of compound 14977614 and compound 63818502 to the FGFR3. In particular, mutating G322 showed a severe reduction for all parameters for both compounds suggesting that the G322 interaction was likely important for activating FGFR3 biological functions. Molecular dynamics (MD) simulations were performed to determine the stability of compound 14977614 in the active site of FGFR3. Computational analysis revealed that the stabilization between FGFR3 and 14977614 occurred between 30 ns and 40 ns. The average backbone RMSD is around 0.15 nm–0.35 nm. The solvent accessible surface area is around 300 nm–360 nm which clearly indicates that the molecule 14977614 can easily access the active site of FGFR3. Furthermore, we have also calculated the number of hydrogen bonds throughout the simulation. We observed an average number of hydrogen bonds are two to five which clearly shows the compounds have close contact with the FGFR3 molecule throughout the simulation period (Figure 1(h) to (j)). Overall, the MD simulation results indicated that the molecule 14977614 is stable throughout the simulation period in the FGFR3 active site.

To determine if the identified compounds are functionally active, we tested the biological activity of 14977614 because it had high oral absorption rate and acceptable range of drug-likeness properties. Based on the known effects of FGFR3-FGF interaction in stimulating osteogenic cell proliferation and differentiation, we tested if the compound, 14977614, exerts a stimulatory effect on

Table 2. Alanine scanning mutagenesis and relative binding free energies (kcal/mol) between wild and mutant FGFR3/-14977614 and FGFR3-63818502 complexes.

Amino acids	Interaction type	Compound	ΔGbind[a] (kcal/mol)	ΔGbind$_{covalent}$[b] (kcal/mol)	ΔGbind$_{Hbond}$[c] (kcal/mol)	ΔGbind$_{Lipo}$[d] (kcal/mol)	ΔGbind$_{SolvGB}$[e] (kcal/mol)
VA277A	Wild type	14977614	−112.46	18.48	−0.89	−116.78	25.82
		63818502	−126.48	15.49	−0.75	−99.12	22.85
	Mutated	14977614	−98.49	10.21	−0.52	−102.54	22.11
		63818502	−110.56	12.10	−0.41	−80.11	19.85
S279A	Wild type	14977614	−112.46	18.48	−0.89	−116.78	25.82
		63818502	−126.48	15.49	−0.75	−99.12	22.85
	Mutated	14977614	−99.61	10.85	−0.58	−95.42	20.19
		63818502	−112.64	11.45	−0.32	−75.12	18.72
L319A	Wild type	14977614	−112.46	18.48	−0.89	−116.78	25.82
		63818502	−126.48	15.49	−0.75	−99.12	22.85
	Mutated	14977614	−100.12	9.82	−0.42	−82.15	18.11
		63818502	−98.54	10.21	−0.12	−70.18	11.31
L321A	Wild type	14977614	−112.46	18.48	−0.89	−116.78	25.82
		63818502	−126.48	15.49	−0.75	−99.12	22.85
	L321A	14977614	−85.12	5.12	0.12	−75.11	10.12
		63818502	−100.48	9.52	−0.18	−69.78	9.87
G322A	Wild type	14977614	−112.46	18.48	−0.89	−116.78	25.82
		63818502	−126.48	15.49	−0.75	−99.12	22.85
	G322A	14977614	−75.56	−2.12	2.51	−51.23	6.85
		63818502	−82.12	−1.12	−0.10	−51.11	4.21

[a]MM/GBSA binding free energy.
[b]Contribution to the MMGBSA free energy of binding from covalent binding.
[c]Contribution to the MMGBSA free energy of binding from hydrogen bonding.
[d]Contribution to the MMGBSA free energy of binding from lipophillic binding.
[e]Contribution to the MMGBSA free energy of binding from the generalized born electrostatic solvation energy.
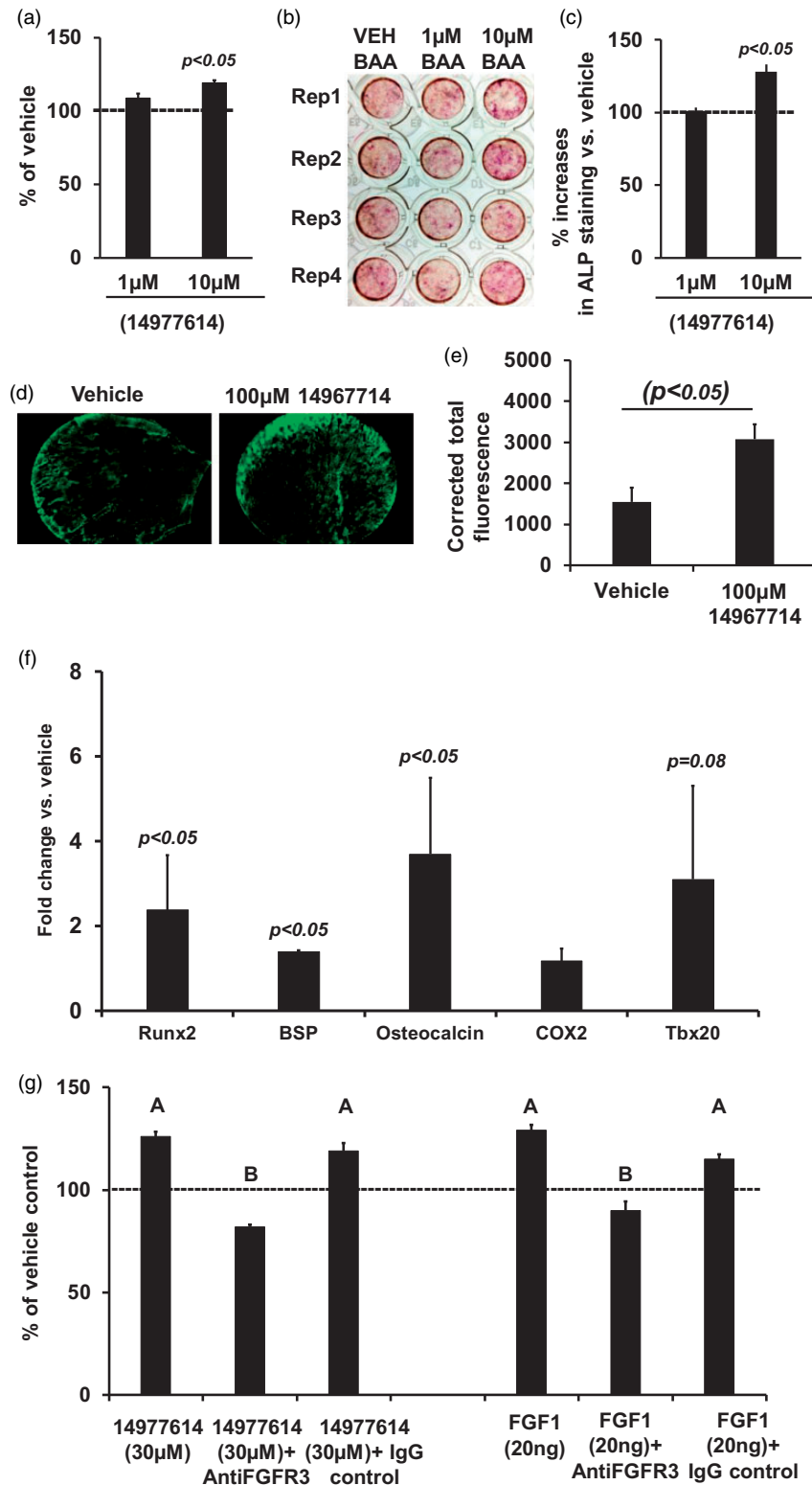
Figure 2. (a) Quantitation of cell number change in BMCs treated with 1 μM and 10 μM 14976614 and (b) Image of ALP staining of BMSCs treated with β-glycer-ophosphate- ascorbic acid (BAA) with varying dose of 14976614 and vehicle (VEH) and (c) quantitative analysis of ALP staining at 590 nM, (d) Microscope image (e) quantitative analysis of calvaria treated with vehicle and 100 μM 14977614 for seven days (40×). The green fluorescence represents mineralization and (f) Quantitation of bone markers by real-time PCR in one-week-old calvaria from C57BL/6J mice cultured *ex vivo* for seven days with treatment of 100 μM dose of compound 14977614 once per day for seven days, and (g) Quantitation of cell number change in BMSCs treated with 30 μM 14976614 or 20 ng/mL of FGF1 in the presences of vehicle, 1 μg/mL of Anti-FGFR3 or 1 μg/mL normal rat IgG. Values are the Mean ± SEM, $n = 5$ mice for proliferation and ALP staining, $n = 3$ mice for mineralization imaging and gene expression, $n = 4$–6/group for Figure 2(g), [A]$P < 0.001$ vs. vehicle control and [B]$P < 0.001$ vs. normal rat IgG. (A color version of this figure is available in the online journal.)

proliferation and differentiation of BMSCs.[7,20] We found that treatment of BMCS with 10 μM 14977614 increased cell number by 20%. While there was a small increase in cell number with the 1 μM dose, this effect was not significant (Figure 2(a)). Figure 2(b) shows that BMCSs treated with 10 μM 14976614 showed increased ALP staining compared to cells treated with vehicle alone when cultured in differentiation medium. Quantitative analysis revealed a 25% increase in ALP staining, reflecting increased differentiation (Figure 2(c)). A similar finding was also observed in the ST2 stromal cell line in which both doses of compound 14976614 increased (10–17%, $P < 0.05$) ALP staining. Consistent with this data, we also found that calvaria treated with 100 μM 14977614 showed increased mineralization as reflected by the increased green fluorescence signal in 14977614 treated culture compared to control culture (Figure 2(d)). Semi-quantitative analysis of the fluorescence revealed increased mineralization, in the calvaria treated with 14977614 (Figure 2(e)). Accordingly, we found that expression levels of bone formation markers, Runx2, BSP, and osteocalcin were significantly increased in calvaria treated with 14977614 (Figure 2(f)). Overall, these data show that the identified compound 14977614 induces both BMSC proliferation and differentiation that are important when considering therapeutic development.

To further determine if the stimulatory effect of 14977614 is mediated via FGFR3, we evaluated the consequence of neutralizing FGFR3 action with Anti-FGFR3 antibody on the mitogenic effects of 14977614 using serum-free cultures of BMSCs. We used 20 ng/mL FGF1 as a positive control based on the evidence that FGF1 interacts FGFR3 to induce cell proliferation. Since rat monoclonal antibody (Anti-FGFR3) was used to neutralize FGFR3 action, we used normal rat IgG as a control to validate the specificity of rat monoclonal antibody used in this study. Our findings demonstrate that small molecule 14977614 stimulated proliferation of BMSCs to a similar extent as that of positive control (FGF1) (Figure 2(g)). Anti-FGFR3 treatment completely blocked the stimulatory effects of 14977614 or FGF1 on BMSC proliferation (Figure 2(g)), suggesting that small molecule or FGF1 is competing with anti-FGFR3 for receptor binding. In contrast, normal rat IgG did not block the stimulatory effects of 14977614 or FGF1 on BMSC proliferation. Together these data suggest that the mitogenic effect of 14977614 on BMSCs mediated largely via FGFR3.

In this study, we examined the biological effects of only one FGFR3 agonist. The remaining six compounds need to be tested to determine which of these compounds exhibit the greatest potential to induce FGFR3 signaling as well as anabolic biological effects on bone cells. Also, we need to examine if downstream targets of FGFR3 are induced by the small molecule FGFR3 agonists identified and if their biological effects can be completely blocked by inhibition of FGFR3 signaling. Future confirmation of the specificity of the identified agonists and confirmation of their biological effects to stimulate bone formation *in vivo* would provide impetus for the use of *in silico* computational analysis with predicted three-dimensional structures of receptors for future identification of agonists for other receptors of interest.

ORCID iD

Chandrasekhar Kesavan https://orcid.org/0000-0003-0685-0367

REFERENCES

1. Cao X, Chen D. The BMP signaling and in vivo bone formation. *Gene* 2005;**357**:1–8
2. Houschyar KS, Tapking C, Borrelli MR, Popp D, Duscher D, Maan ZN, Chelliah MP, Li J, Harati K, Wallner C, Rein S, Pforringer D, Reumuth G, Grieb G, Mouraret S, Dadras M, Wagner JM, Cha JY, Siemers F, Lehnhardt M, Behr B. Wnt pathway in bone repair and regeneration – what do we know so far. *Front Cell Dev Biol* 2018;**6**:170
3. Kawai M, Rosen CJ. The insulin-like growth factor system in bone: basic and clinical implications. *Endocrinol Metab Clin North Am* 2012;**41**:323–33, vi
4. Nan S, Min J, Lin C. Role of FGF/FGFR signaling in skeletal development and homeostasis: learning from mouse models. *Bone Res* 2014;**2**:14003
5. Mengrui W, Guiquian C, Yi-Ping L. TGF-beta and BMP signaling in osteoblast, skeletal development, and bone formation, homeostasis and disease. *Bone Res* 2016;**4**:16009–30
6. Zhong Z, Ethen NJ, Williams BO. WNT signaling in bone development and homeostasis. *Wiley Interdisc Rev Dev Biol* 2014;**3**:489–500
7. Emilie D, Ivan K, Alesandro B, Ghaith A, Joanne E, Marine L, Imke F, Olivia B, E, Elizabeth P, Bjorn B, Mickael M, Frederic S, Laurence LM. Fgfr3 is a positive regulator of osteoblast expansion and differentiation during zebrafish skull vault development. *J Bone Miner Res* 2020;**35**:1782–97
8. Nan S, Qidi S, Can L, Xiumin L, Huabing Q, Siyu C, Jing Y, Xiaolan D, Ling Z, Qifen H, Min J, Yue S, Di C, Lin C. Gain-of-function mutation in FGFR3 in mice leads to decreased bone mass by affecting both osteoblastogenesis and osteoclastogenesis. *Hum Mol Genet* 2010;**19**:1199–210

9. Lee YC, Song IW, Pai YJ, Chen SD, Chen YT. Knock-in human FGFR3 achondroplasia mutation as a mouse model for human skeletal dysplasia. *Sci Rep* 2017;**7**:43220

10. Schmid GJ, Kobayashi C, Sandell LJ, Ornitz DM. Fibroblast growth factor expression during skeletal fracture healing in mice. *Dev Dyn* 2009;**238**:766–74

11. Olsen SK, Ibrahimi OA, Raucci A, Zhang F, Eliseenkova AV, Yayon A, Basilico C, Linhardt RJ, Schlessinger J, Mohammadi M. Insights into the molecular basis for fibroblast growth factor receptor autoinhibition and ligand-binding promiscuity. *Proc Natl Acad Sci U S A* 2004;**101**:935–40

12. Peach ML, Zakharov AV, Liu R, Pugliese A, Tawa G, Wallqvist A, Nicklaus MC. Computational tools and resources for metabolism-related property predictions. 1. Overview of publicly available (free and commercial) databases and software. *Future Med Chem* 2012;**4**:1907–32

13. Qidwai T. QSAR modeling, docking and ADMET studies for exploration of potential anti-malarial compounds against Plasmodium falciparum. *In Silico Pharmacol* 2016;**5**:6–24

14. Lee C, Yang W, Parr RG. Development of the Colle-Salvetti correlation-energy formula into a functional of the electron density. *Phys Rev B Condens Matter* 1988;**37**:785–9

15. Nagamani S, Kesavan C, Muthusamy K. Atom-based and pharmacophore-based 3D – QSAR studies on vitamin D receptor (VDR). *Comb Chem High Throughput Screen* 2018;**21**:329–43

16. Nagamani S, Muthusamy K. A theoretical insight to understand the molecular mechanism of dual target ligand CTA-018 in the chronic kidney disease pathogenesis. *PLoS One* 2018;**13**:e0203194

17. Lindsey RC, Mohan S. Thyroid hormone acting via TRbeta induces expression of browning genes in mouse bone marrow adipose tissue. *Endocrine* 2017;**56**:109–20

18. Kwist K, Bridges WC, Burg KJ. The effect of cell passage number on osteogenic and adipogenic characteristics of D1 cells. *Cytotechnology* 2016;**68**:1661–7

19. Kesavan C, Baylink DJ, Kapoor S, Mohan S. Novel loci regulating bone anabolic response to loading: expression QTL analysis in C57BL/6JXC3H/HeJ mice cross. *Bone* 2007;**41**:223–30

20. Ueno N, Shimizu A, Kanai M, Iwaya Y, Ueda S, Nakayama J, Seo MK. Enhanced expression of fibroblast growth factor receptor 3 IIIc promotes human esophageal carcinoma cell proliferation. *J Histochem Cytochem* 2016;**64**:7–17